

Hadronic Vacuum Polarization in the Spacelike Region and the MUonE Experiment

Gilberto Colangelo

u^b

b
UNIVERSITÄT
BERN

AEC
ALBERT EINSTEIN CENTER
FOR FUNDAMENTAL PHYSICS

MUonE topical Workshop – MITP Mainz, November 17

Outline

Introduction: $(g - 2)_\mu$ in the Standard Model

Lattice vs data-driven approach

- Lattice HVP and intermediate window

- Data-driven approach

- Dispersive approach for the $\pi\pi$ contribution

Spacelike region and MUonE

Master Thesis of Barbara Jenny

Conclusions

Outline

Introduction: $(g - 2)_\mu$ in the Standard Model

Lattice vs data-driven approach

Lattice HVP and intermediate window

Data-driven approach

Dispersive approach for the $\pi\pi$ contribution

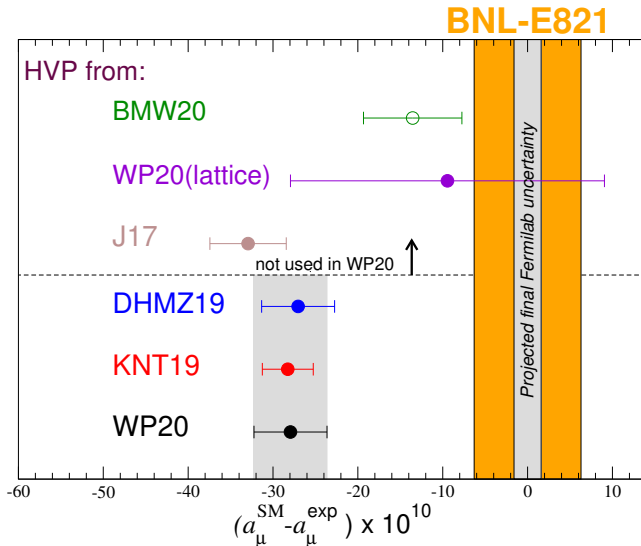
Spacelike region and MUonE

Master Thesis of Barbara Jenny

Conclusions

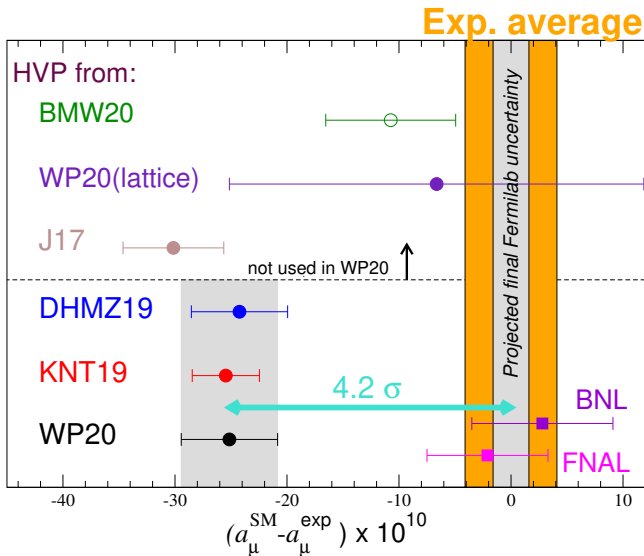
Present status of $(g - 2)_\mu$: experiment vs SM

Before



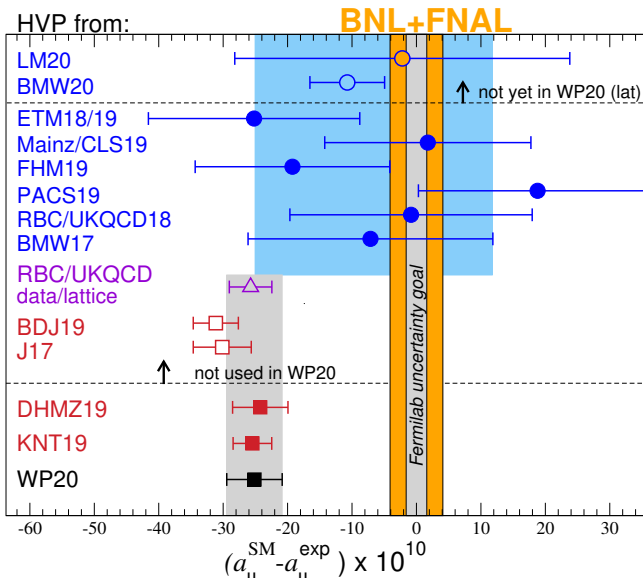
Present status of $(g - 2)_\mu$: experiment vs SM

After the Fermilab result



Present status of $(g - 2)_\mu$: experiment vs SM

After the Fermilab result



White Paper (2020): $(g - 2)_\mu$, experiment vs SM

| Contribution | Value $\times 10^{11}$ |
|--|------------------------|
| HVP LO ($e^+ e^-$) | 6931(40) |
| HVP NLO ($e^+ e^-$) | -98.3(7) |
| HVP NNLO ($e^+ e^-$) | 12.4(1) |
| HVP LO (lattice , $udsc$) | 7116(184) |
| HLbL (phenomenology) | 92(19) |
| HLbL NLO (phenomenology) | 2(1) |
| HLbL (lattice, uds) | 79(35) |
| HLbL (phenomenology + lattice) | 90(17) |
| QED | 116 584 718.931(104) |
| Electroweak | 153.6(1.0) |
| HVP ($e^+ e^-$, LO + NLO + NNLO) | 6845(40) |
| HLbL (phenomenology + lattice + NLO) | 92(18) |
| Total SM Value | 116 591 810(43) |
| Experiment | 116 592 061(41) |
| Difference: $\Delta a_\mu := a_\mu^{\text{exp}} - a_\mu^{\text{SM}}$ | 251(59) |

White Paper (2020): $(g - 2)_\mu$, experiment vs SM

| Contribution | Value $\times 10^{11}$ |
|--|------------------------|
| HVP LO ($e^+ e^-$) | 6931(40) |
| HVP NLO ($e^+ e^-$) | -98.3(7) |
| HVP NNLO ($e^+ e^-$) | 12.4(1) |
| HVP LO (lattice BMW(20) , <i>udsc</i>) | 7075(55) |
| HLbL (phenomenology) | 92(19) |
| HLbL NLO (phenomenology) | 2(1) |
| HLbL (lattice, <i>uds</i>) | 79(35) |
| HLbL (phenomenology + lattice) | 90(17) |
| QED | 116 584 718.931(104) |
| Electroweak | 153.6(1.0) |
| HVP ($e^+ e^-$, LO + NLO + NNLO) | 6845(40) |
| HLbL (phenomenology + lattice + NLO) | 92(18) |
| Total SM Value | 116 591 810(43) |
| Experiment | 116 592 061(41) |
| Difference: $\Delta a_\mu := a_\mu^{\text{exp}} - a_\mu^{\text{SM}}$ | 251(59) |

White Paper (2020): $(g - 2)_\mu$, experiment vs SM

White Paper:

T. Aoyama et al. Phys. Rep. 887 (2020) = WP(20)

Muon $g - 2$ Theory Initiative

Steering Committee:

GC

Michel Davier (vice-chair)

Aida El-Khadra (chair)

Martin Hoferichter

Laurent Lellouch

Christoph Lehner (vice-chair)

Tsutomu Mibe (J-PARC E34 experiment)

Lee Roberts (Fermilab E989 experiment)

Thomas Teubner

Hartmut Wittig

White Paper (2020): $(g - 2)_\mu$, experiment vs SM

White Paper:

T. Aoyama et al. Phys. Rep. 887 (2020) = WP(20)

Muon $g - 2$ Theory Initiative

Workshops:

- ▶ 1st plenary meeting, Q-Center (Fermilab), 3-6 June 2017
- ▶ 2nd plenary meeting, Mainz, 18-22 June 2018
- ▶ 3rd plenary meeting, Seattle, 9-13 September 2019
- ▶ Lattice HVP workshop, virtual, 16-20 November 2020
- ▶ 4th plenary meeting, KEK (virtual), 28 June-02 July 2021
- ▶ 5th plenary meeting, Higgs Center Edinburgh, 5-9 Sept. 2022
- ▶ 6th plenary meeting, A. Einstein Center Bern, (4-8 Sept. 2023)

White Paper executive summary (my own)

- ▶ QED and EW known and stable, negligible uncertainties
- ▶ HVP dispersive: consensus number, conservative uncertainty (KNT19, DHMZ19, CHS19, HHK19)
- ▶ HVP lattice: consensus number, $\Delta a_\mu^{\text{HVP,latt}} \sim 5 \Delta a_\mu^{\text{HVP,disp}}$
(Fermilab-HPQCD-MILC18,20, BMW18, RBC/UKQCD18, ETM19,SK19, Mainz19, ABTGJP20)
- ▶ HVP BMW20: central value \rightarrow discrepancy $< 2\sigma$;
 $\Delta a_\mu^{\text{HVP,BMW}} \sim \Delta a_\mu^{\text{HVP,disp}}$ published 04/21 \rightarrow not in WP
- ▶ HLbL dispersive: consensus number, w/ recent improvements $\Rightarrow \Delta a_\mu^{\text{HLbL}} \sim 0.5 \Delta a_\mu^{\text{HVP}}$
- ▶ HLbL lattice: single calculation, agrees with dispersive
($\Delta a_\mu^{\text{HLbL,latt}} \sim 2 \Delta a_\mu^{\text{HLbL,disp}}$) \rightarrow final average (RBC/UKQCD20)

Outline

Introduction: $(g - 2)_\mu$ in the Standard Model

Lattice vs data-driven approach

Lattice HVP and intermediate window

Data-driven approach

Dispersive approach for the $\pi\pi$ contribution

Spacelike region and MUonE

Master Thesis of Barbara Jenny

Conclusions

The BMW result

Borsanyi et al. Nature 2021

State-of-the-art lattice calculation of $a_\mu^{\text{HVP, LO}}$ based on

- ▶ current-current correlator, summed over all distances, integrated in time with appropriate kernel function (TMR)
- ▶ using staggered fermions on an $L \sim 6$ fm lattice ($L \sim 11$ fm used for finite volume corrections)
- ▶ at (and around) physical quark masses
- ▶ including isospin-breaking effects

The BMW result

Borsanyi et al. Nature 2021

Isospin-symmetric



Connected light

$$633.7(2.1)_{\text{stat}}(4.2)_{\text{sys}}$$



Connected strange

$$53.393(89)_{\text{stat}}(68)_{\text{sys}}$$



Connected charm

$$14.6(0)_{\text{stat}}(1)_{\text{sys}}$$



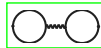
Disconnected

$$-13.36(1.18)_{\text{stat}}(1.36)_{\text{sys}}$$

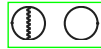
QED isospin breaking: valence



$$\text{Connected } -1.23(40)_{\text{stat}}(31)_{\text{sys}}$$



$$\text{Disconnected } -0.55(15)_{\text{stat}}(10)_{\text{sys}}$$



Strong-isospin breaking



Connected

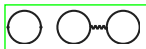
$$6.60(63)_{\text{stat}}(53)_{\text{sys}}$$



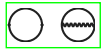
Disconnected

$$-4.67(54)_{\text{stat}}(69)_{\text{sys}}$$

QED isospin breaking: sea



$$\text{Connected } 0.37(21)_{\text{stat}}(24)_{\text{sys}}$$



$$\text{Disconnected } -0.040(33)_{\text{stat}}(21)_{\text{sys}}$$



Other

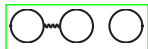
Bottom; higher-order;
perturbative

$$0.11(4)_{\text{tot}}$$

QED isospin breaking: mixed



$$\text{Connected } -0.0093(86)_{\text{stat}}(95)_{\text{sys}}$$



$$\text{Disconnected } 0.011(24)_{\text{stat}}(14)_{\text{sys}}$$

Finite-size effects

Isospin-symmetric

$$18.7(2.5)_{\text{tot}}$$

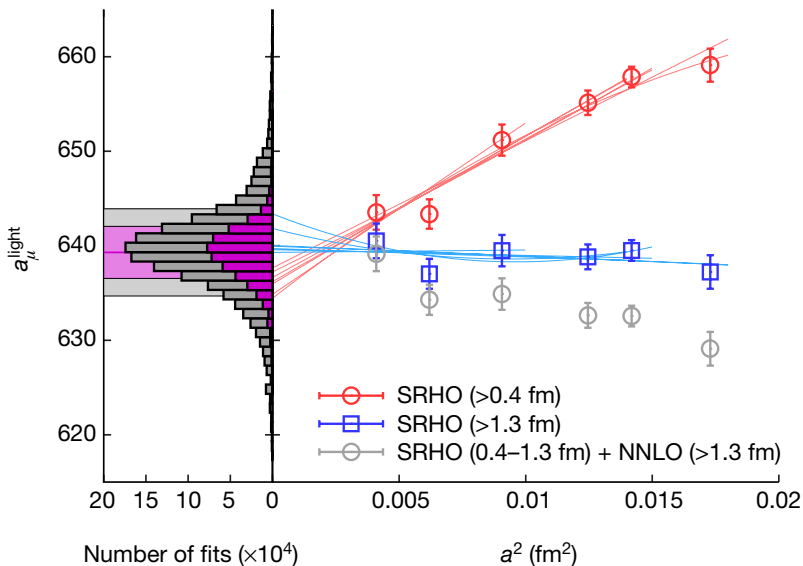
Isospin-breaking

$$0.0(0.1)_{\text{tot}}$$

$$a_{\mu}^{\text{LO-HVP}} (\times 10^{10}) = 707.5(2.3)_{\text{stat}}(5.0)_{\text{sys}}(5.5)_{\text{tot}}$$

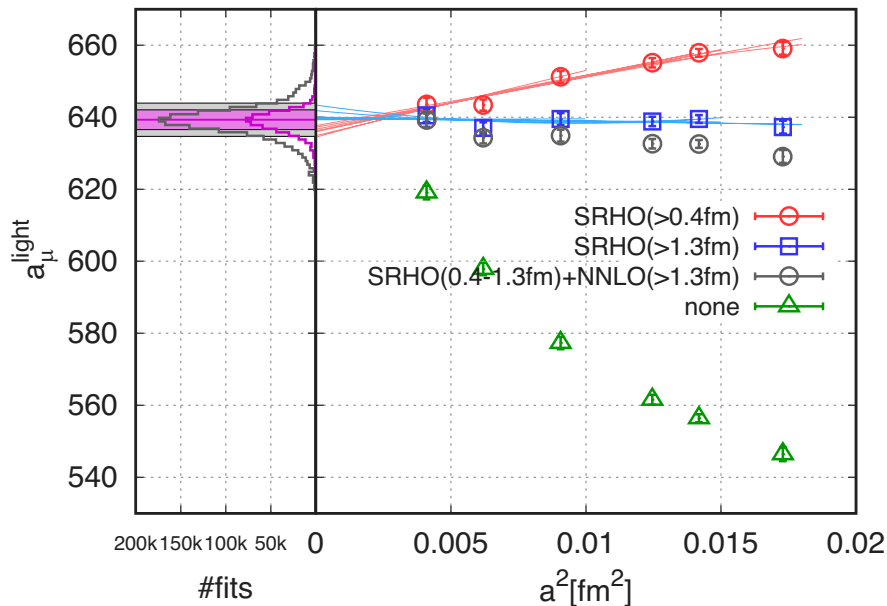
The BMW result

Borsanyi et al. Nature 2021



The BMW result

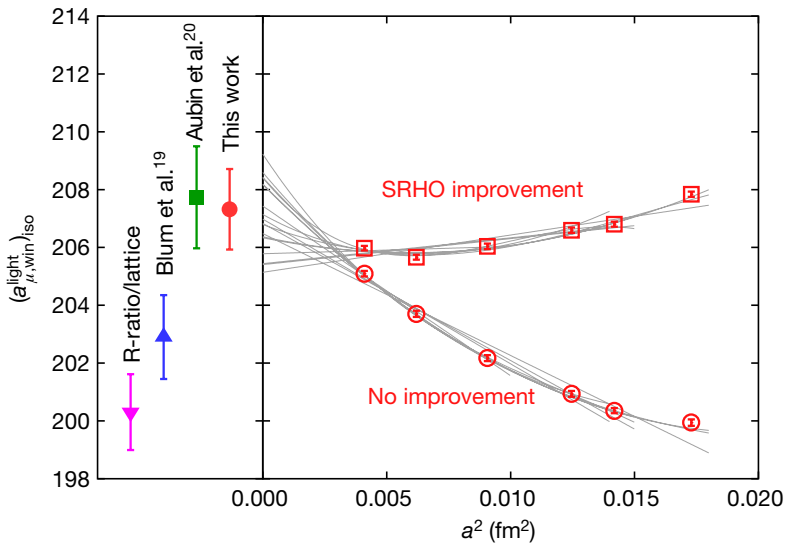
Borsanyi et al. Nature 2021



The BMW result

Borsanyi et al. Nature 2021

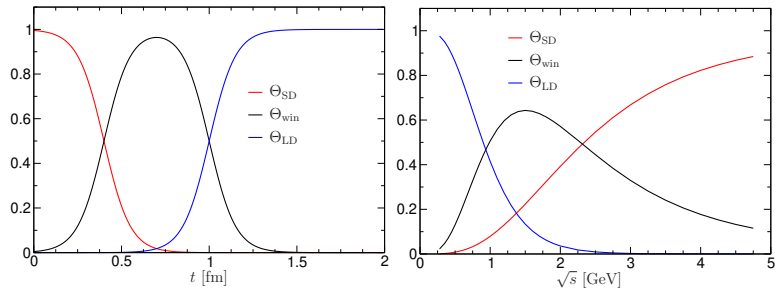
Article



The BMW result

Borsanyi et al. Nature 2021

Weight functions for window quantities

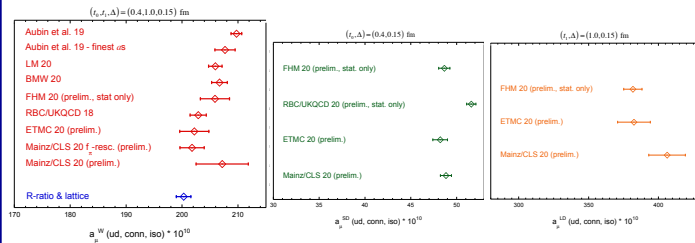


The BMW result

Borsanyi et al. Nature 2021

Summary: ud contribution

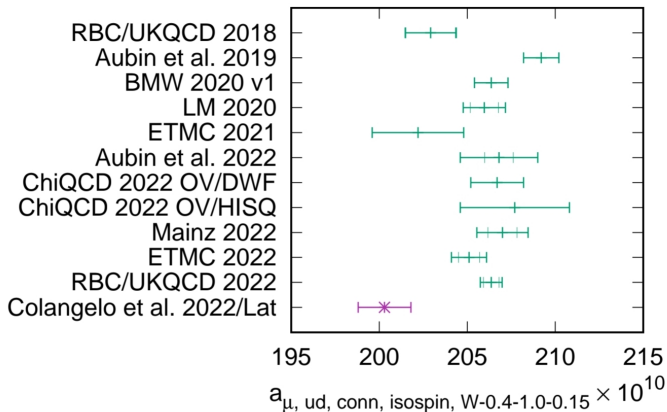
| f | $a_\mu^{SD}(f) \cdot 10^{10}$ | $a_\mu^W(f) \cdot 10^{10}$ | $a_\mu^{LD}(f) \cdot 10^{10}$ |
|------|-------------------------------|----------------------------|-------------------------------|
| ud | 48.2 (0.8) | 202.2 (2.6) | 382.5 (11.7) |



13

Present status of the window quantities

Several lattice calculations now confirm BMW's result

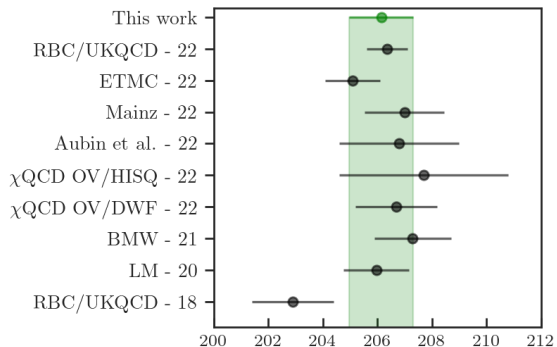


R-ratio: GC, El-Khadra, Hoferichter, Keshavarzi, Lehner, Stoffer, Teubner (22)

Plot by C. Lehner, Edinburgh 2022

Present status of the window quantities

Several lattice calculations now confirm BMW's result



Individual-channel contributions to a_μ^{win}

| Channel | total | window |
|---|--------------|------------|
| $\pi^+\pi^-$ | 504.23(1.90) | 144.08(49) |
| $\pi^+\pi^-\pi^0$ | 46.63(94) | 18.63(35) |
| $\pi^+\pi^-\pi^+\pi^-$ | 13.99(19) | 8.88(12) |
| $\pi^+\pi^-\pi^0\pi^0$ | 18.15(74) | 11.20(46) |
| K^+K^- | 23.00(22) | 12.29(12) |
| $K_S K_L$ | 13.04(19) | 6.81(10) |
| $\pi^0\gamma$ | 4.58(10) | 1.58(4) |
| Sum of the above | 623.62(2.27) | 203.47(78) |
| [1.8, 3.7] GeV (without $c\bar{c}$) | 34.45(56) | 15.93(26) |
| $J/\psi, \psi(2S)$ | 7.84(19) | 2.27(6) |
| [3.7, ∞) GeV | 16.95(19) | 1.56(2) |
| WP(20) / GC, El-Khadra <i>et al.</i> (22) | 693.1(4.0) | 229.4(1.4) |
| BMWc | 707.5(5.5) | 236.7(1.4) |
| Mainz/CLS | | 237.3(1.5) |
| ETMc | | 235.0(1.1) |
| RBC/UKQCD | | 235.6(0.8) |

Numbers for the channels refer to KNT19 — thanks to Alex Keshavarzi for providing them

$$\Delta a_\mu^{\text{HVP, LO}} = 14.4(6.8) (2.1\sigma), \quad \Delta a_\mu^{\text{win}} \sim 6.5(1.5) (\sim 4.3\sigma)$$

Hadronic vacuum polarization

$$\Pi_{\mu\nu}(q) = i \int d^4x e^{iqx} \langle 0 | T j_\mu(x) j_\nu(0) | 0 \rangle = (q_\mu q_\nu - g_{\mu\nu} q^2) \Pi(q^2)$$

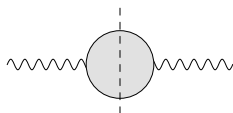
where $j^\mu(x) = \sum_i Q_i \bar{q}_i(x) \gamma^\mu q_i(x)$, $i = u, d, s$ is the em current

- ▶ Lorentz invariance: 2 structures
- ▶ gauge invariance: reduction to 1 structure
- ▶ Lorentz-tensor defined in such a way that the function $\Pi(q^2)$ does not have kinematic singularities or zeros
- ▶ $\bar{\Pi}(q^2) := \Pi(q^2) - \Pi(0)$ satisfies

$$\bar{\Pi}(q^2) = \frac{q^2}{\pi} \int_{4M_\pi^2}^{\infty} dt \frac{\text{Im}\bar{\Pi}(t)}{t(t - q^2)}$$

HVP contribution: Master Formula

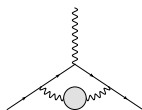
Unitarity relation: **simple**, same for all intermediate states



$$\text{Im}\bar{\Pi}(q^2) \propto \sigma(e^+e^- \rightarrow \text{hadrons}) = \sigma(e^+e^- \rightarrow \mu^+\mu^-)R(q^2)$$

Analyticity $\left[\bar{\Pi}(q^2) = \frac{q^2}{\pi} \int ds \frac{\text{Im}\bar{\Pi}(s)}{s(s-q^2)} \right] \Rightarrow$ **Master formula for HVP**

Bouchiat, Michel (61)



\Leftrightarrow

$$a_{\mu}^{\text{hvp}} = \frac{\alpha^2}{3\pi^2} \int_{s_{\text{th}}}^{\infty} \frac{ds}{s} K(s)R(s)$$

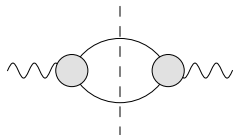
$K(s)$ known, depends on m_{μ} and $K(s) \sim \frac{1}{s}$ for large s

Comparison between DHMZ19 and KNT19

| | DHMZ19 | KNT19 | Difference |
|--------------------------------------|--|--------------|------------|
| $\pi^+\pi^-$ | 507.85(0.83)(3.23)(0.55) | 504.23(1.90) | 3.62 |
| $\pi^+\pi^-\pi^0$ | 46.21(0.40)(1.10)(0.86) | 46.63(94) | -0.42 |
| $\pi^+\pi^-\pi^+\pi^-$ | 13.68(0.03)(0.27)(0.14) | 13.99(19) | -0.31 |
| $\pi^+\pi^-\pi^0\pi^0$ | 18.03(0.06)(0.48)(0.26) | 18.15(74) | -0.12 |
| K^+K^- | 23.08(0.20)(0.33)(0.21) | 23.00(22) | 0.08 |
| $K_S K_L$ | 12.82(0.06)(0.18)(0.15) | 13.04(19) | -0.22 |
| $\pi^0\gamma$ | 4.41(0.06)(0.04)(0.07) | 4.58(10) | -0.17 |
| Sum of the above | 626.08(0.95)(3.48)(1.47) | 623.62(2.27) | 2.46 |
| [1.8, 3.7] GeV (without $c\bar{c}$) | 33.45(71) | 34.45(56) | -1.00 |
| $J/\psi, \psi(2S)$ | 7.76(12) | 7.84(19) | -0.08 |
| [3.7, ∞) GeV | 17.15(31) | 16.95(19) | 0.20 |
| Total $a_\mu^{\text{HVP, LO}}$ | 694.0(1.0)(3.5)(1.6)(0.1) $_{\psi(0.7)_{\text{DV+QCD}}}$ | 692.8(2.4) | 1.2 |

The 2π contribution

For HVP the unitarity relation is **simple** and looks the same for all possible intermediate states, like 2π



$$\text{Im}\Pi(q^2) \propto \sigma(e^+e^- \rightarrow \pi^+\pi^-)$$

which implies

$$\bar{\Pi}_{2\pi}(q^2) = \frac{q^2}{\pi} \int_{4M_\pi^2}^{\infty} dt \frac{\alpha\sigma_\pi(t)^3 |F_V^\pi(t)|^2}{12t(t-q^2)}$$

de Trocóniz, Ynduráin (01,04), Leutwyler, GC (02,03), Anhanarayan et al. (13,16)

The pion vector form factor $F_V^\pi(t)$ also satisfies a dispersion relation

Analytic properties of pion form factors

Mathematical problem:

1. $F(t)$: analytic function except for a cut for $4M_\pi^2 \leq t < \infty$
2. $e^{-i\delta(t)}F(t) \in \mathbb{R}$ for $\text{Im}(t) \rightarrow 0^+$, with $\delta(t)$ a known function

Exact solution:

Omnès (58)

$$F(t) = P(t)\Omega(t) = P(t) \exp \left\{ \frac{t}{\pi} \int_{4M_\pi^2}^{\infty} \frac{dt'}{t'} \frac{\delta(t')}{t' - t} \right\},$$

$P(t)$ a polynomial \Leftrightarrow behaviour of $F(t)$ for $t \rightarrow \infty$
or presence of zeros

$\Omega(t)$ is called the Omnès function

Vector form factor of the pion

Pion vector form factor

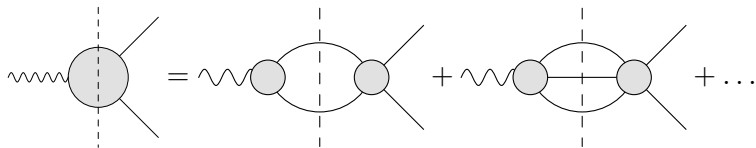
$$\langle \pi^i(p') | V_\mu^k(0) | \pi^l(p) \rangle = i \epsilon^{ikl} (p' + p)_\mu F_V^\pi(s) \quad s = (p' - p)^2$$

- ▶ normalization fixed by gauge invariance:

$$F_V^\pi(0) = 1 \quad \xrightarrow{\text{no zeros}} \quad P(t) = 1$$

- ▶ $e^+e^- \rightarrow \pi^+\pi^-$ data \Rightarrow free parameters in $\Omega(t)$

Omnès representation including isospin breaking



Omnès representation including isospin breaking

- ▶ Omnès representation

$$F_V^\pi(s) = \exp \left[\frac{s}{\pi} \int_{4M_\pi^2}^{\infty} ds' \frac{\delta(s')}{s'(s'-s)} \right] \equiv \Omega(s)$$

- ▶ Split **elastic** ($\leftrightarrow \pi\pi$ phase shift, δ_1^1) from **inelastic** phase

$$\delta = \delta_1^1 + \delta_{\text{in}} \quad \Rightarrow \quad F_V^\pi(s) = \Omega_1^1(s) \Omega_{\text{in}}(s)$$

Eidelman-Lukaszuk: unitarity bound on δ_{in}

$$\sin^2 \delta_{\text{in}} \leq \frac{1}{2} \left(1 - \sqrt{1 - r^2} \right), \quad r = \frac{\sigma_{e^+e^- \rightarrow \neq 2\pi}^{l=1}}{\sigma_{e^+e^- \rightarrow 2\pi}} \Rightarrow s_{\text{in}} = (M_\pi + M_\omega)^2$$

- ▶ **$\rho - \omega$ -mixing** $F_V(s) = \Omega_{\pi\pi}(s) \cdot \Omega_{\text{in}}(s) \cdot G_\omega(s)$

$$G_\omega(s) = 1 + \epsilon \frac{s}{s_\omega - s} \quad \text{where} \quad s_\omega = (M_\omega - i\Gamma_\omega/2)^2$$

Free parameters

$$\Omega_1^1(s) \Rightarrow \begin{cases} \phi_0 = \delta_{\pi\pi}((0.8 \text{ GeV})^2) \\ \phi_1 = \delta_{\pi\pi}(68 M_\pi^2) \end{cases}$$

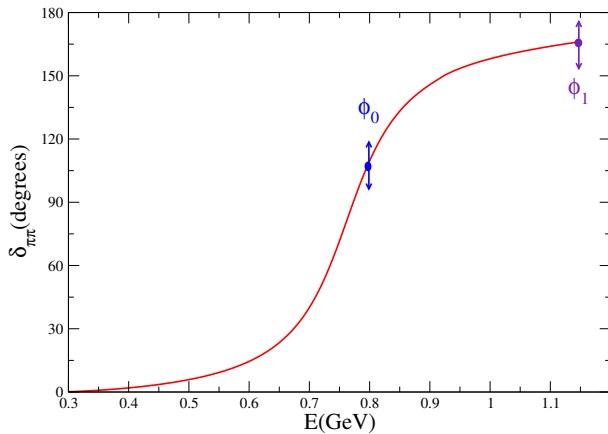
$$G_\omega(s) \Rightarrow \begin{cases} \epsilon & \omega - \rho \text{ mixing} \\ M_\omega \end{cases}$$

$$\Omega_{\text{in}}(s) \Rightarrow \begin{cases} c_1 \\ \vdots \\ c_P \end{cases} \quad \text{Im}\Omega_{\text{in}}(s) = 0 \quad s \leq s_{\text{in}}$$

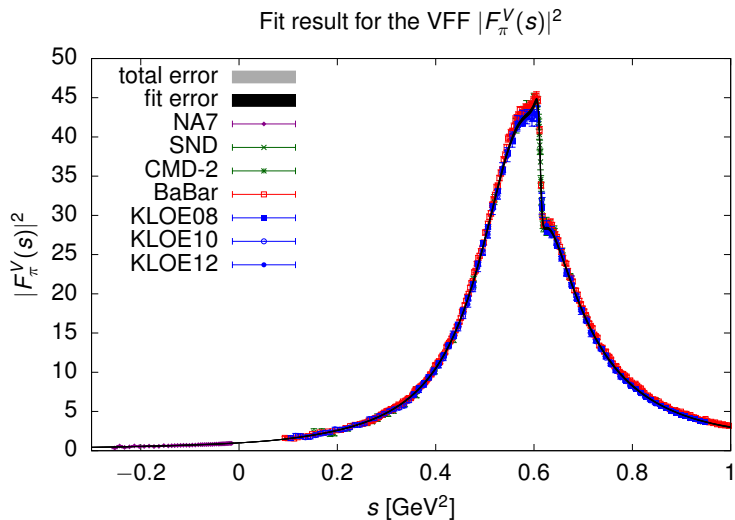
$$G_\omega(s) = 1 + \epsilon \frac{s}{s_\omega - s} \quad \text{where} \quad s_\omega = (M_\omega - i\Gamma_\omega/2)^2$$

$$\Omega_{\text{in}}(s) = 1 + \sum_{k=1}^N c_k (z(s)^k - z(0)^k) \quad z = \frac{\sqrt{s_{\pi\omega} - s_1} - \sqrt{s_{\pi\omega} - s}}{\sqrt{s_{\pi\omega} - s_1} + \sqrt{s_{\pi\omega} - s}}$$

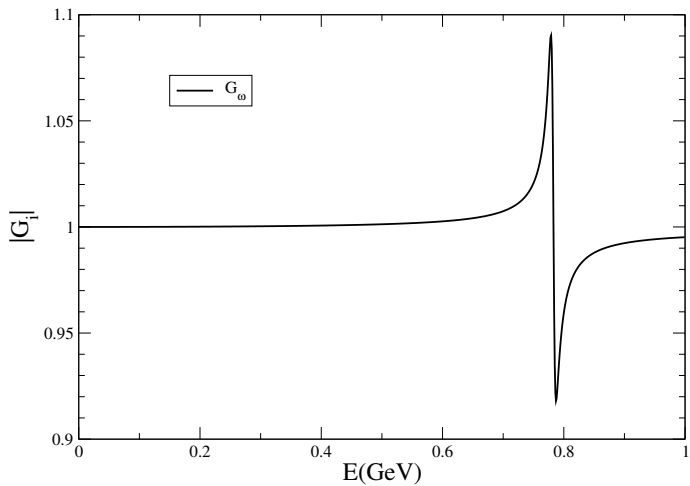
Free parameters



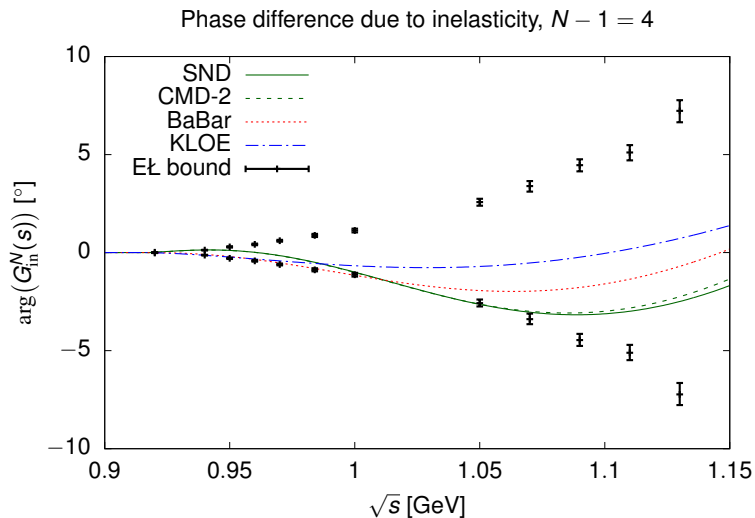
Fit results



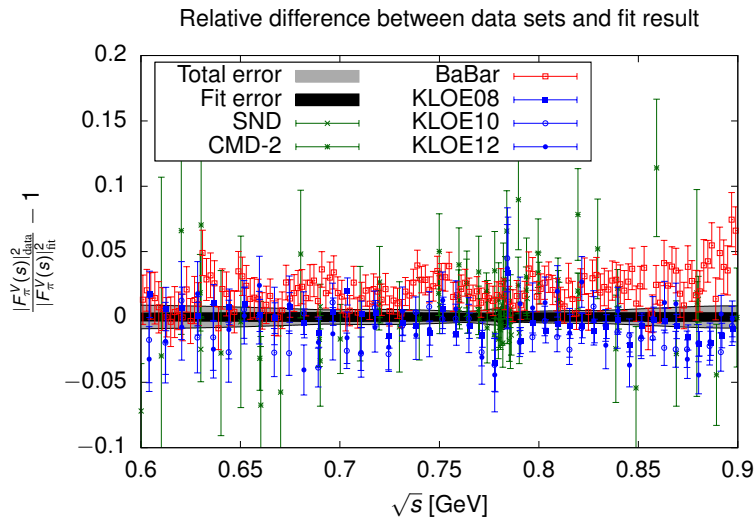
Fit results

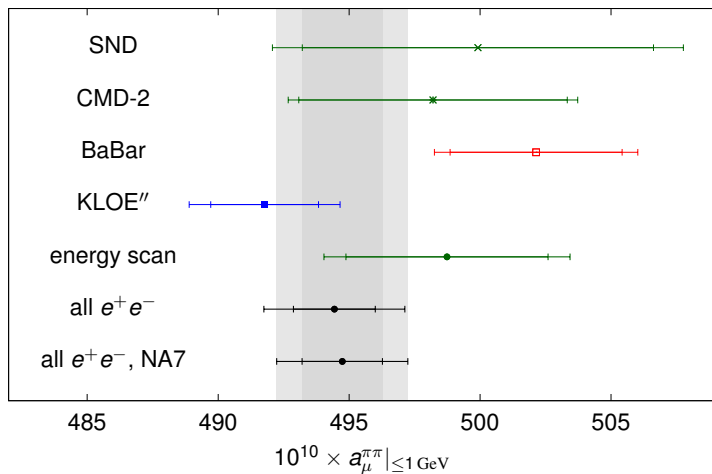


Fit results



Fit results



Results for $(g - 2)_\mu$ Result for $a_\mu^{\pi\pi} |_{\leq 1 \text{ GeV}}$ from the VFF fits to single experiments and combinations

2π : comparison with the dispersive approach

The 2π channel can itself be described dispersively \Rightarrow more constrained theoretically

Ananthanarayan, Caprini, Das (19), GC, Hoferichter, Stoffer (18)

| Energy range | ACD18 | CHS18 | DHMZ19 | KNT19 |
|---------------------------------|----------|------------|-----------------|------------|
| < 0.6 GeV | | 110.1(9) | 110.4(4)(5) | 108.7(9) |
| < 0.7 GeV | | 214.8(1.7) | 214.7(0.8)(1.1) | 213.1(1.2) |
| < 0.8 GeV | | 413.2(2.3) | 414.4(1.5)(2.3) | 412.0(1.7) |
| < 0.9 GeV | | 479.8(2.6) | 481.9(1.8)(2.9) | 478.5(1.8) |
| < 1.0 GeV | | 495.0(2.6) | 497.4(1.8)(3.1) | 493.8(1.9) |
| [0.6, 0.7] GeV | | 104.7(7) | 104.2(5)(5) | 104.4(5) |
| [0.7, 0.8] GeV | | 198.3(9) | 199.8(0.9)(1.2) | 198.9(7) |
| [0.8, 0.9] GeV | | 66.6(4) | 67.5(4)(6) | 66.6(3) |
| [0.9, 1.0] GeV | | 15.3(1) | 15.5(1)(2) | 15.3(1) |
| ≤ 0.63 GeV | 132.9(8) | 132.8(1.1) | 132.9(5)(6) | 131.2(1.0) |
| [0.6, 0.9] GeV | | 369.6(1.7) | 371.5(1.5)(2.3) | 369.8(1.3) |
| $[\sqrt{0.1}, \sqrt{0.95}]$ GeV | | 490.7(2.6) | 493.1(1.8)(3.1) | 489.5(1.9) |

2π : comparison with the dispersive approach

The 2π channel can itself be described dispersively \Rightarrow more constrained theoretically

Ananthanarayan, Caprini, Das (19), GC, Hoferichter, Stoffer (18)

| Energy range | ACD18 | CHS18 | DHMZ19 | KNT19 |
|---------------------------------|----------|------------|-----------------|------------|
| < 0.6 GeV | | 110.1(9) | 110.4(4)(5) | 108.7(9) |
| < 0.7 GeV | | 214.8(1.7) | 214.7(0.8)(1.1) | 213.1(1.2) |
| < 0.8 GeV | | 413.2(2.3) | 414.4(1.5)(2.3) | 412.0(1.7) |
| < 0.9 GeV | | 479.8(2.6) | 481.9(1.8)(2.9) | 478.5(1.8) |
| < 1.0 GeV | | 495.0(2.6) | 497.4(1.8)(3.1) | 493.8(1.9) |
| [0.6, 0.7] GeV | | 104.7(7) | 104.2(5)(5) | 104.4(5) |
| [0.7, 0.8] GeV | | 198.3(9) | 199.8(0.9)(1.2) | 198.9(7) |
| [0.8, 0.9] GeV | | 66.6(4) | 67.5(4)(6) | 66.6(3) |
| [0.9, 1.0] GeV | | 15.3(1) | 15.5(1)(2) | 15.3(1) |
| ≤ 0.63 GeV | 132.9(8) | 132.8(1.1) | 132.9(5)(6) | 131.2(1.0) |
| [0.6, 0.9] GeV | | 369.6(1.7) | 371.5(1.5)(2.3) | 369.8(1.3) |
| $[\sqrt{0.1}, \sqrt{0.95}]$ GeV | | 490.7(2.6) | 493.1(1.8)(3.1) | 489.5(1.9) |

WP(20)

Can the same approach be useful also in the spacelike region?

Outline

Introduction: $(g - 2)_\mu$ in the Standard Model

Lattice vs data-driven approach

Lattice HVP and intermediate window

Data-driven approach

Dispersive approach for the $\pi\pi$ contribution

Spacelike region and MUonE

Master Thesis of Barbara Jenny

Conclusions

Splitting of the polarization function

Analyticity:

$$\bar{\Pi}(t) = \frac{t}{\pi} \int_{s_{th}}^{\infty} ds \frac{\text{Im}\bar{\Pi}(s)}{s(s-t)}$$

Unitarity:

$$\text{Im}\bar{\Pi}(s) = \sum_h \text{Im}\bar{\Pi}_h(s) = \frac{s}{4\pi\alpha} \sigma(e^+e^- \rightarrow h) \quad h = \pi\pi, 3\pi, 4\pi, \dots$$

$$\text{Im}\bar{\Pi}_{\pi\pi}(s) = \frac{\alpha}{12s} \sigma_{\pi}^3(s) |F_{\pi}^V(s)|^2, \dots$$

Therefore:

$$\bar{\Pi}(t) = \sum_h \bar{\Pi}_h(t), \quad \bar{\Pi}_h(t) = \frac{t}{\pi} \int_{s_{th}^h}^{\infty} ds \frac{\text{Im}\bar{\Pi}_h(s)}{s(s-t)}$$

$$s_{th}^{\pi\pi} = 4M_{\pi}^2, \quad s_{th}^{3\pi} \simeq M_{\omega}^2, \quad s_{th}^{4\pi} \simeq (M_{\omega} + M_{\pi})^2, \dots$$

HVP contribution to a_μ – from the spacelike region

Switching from time- to spacelike for $\Pi(s)$:

$$a_\mu^{\text{HVP, LO}} = \frac{\alpha}{\pi^2} \int_{s_{\text{th}}}^{\infty} ds \frac{K(s)}{s} \text{Im} \bar{\Pi}(s) = -\frac{\alpha}{\pi} \int_0^1 dx (1-x) \bar{\Pi}(t(x))$$

where

$$t(x) = -\frac{x^2 m_\mu^2}{1-x}$$

Compare contributions to a_μ through the integrand:

$$(1-x) \bar{\Pi}_h(t(x)) = -\frac{1-x}{\pi} \int_{y_{\text{th}}^h}^{\infty} \frac{dy}{y} \frac{\text{Im} \bar{\Pi}_h(m_\mu^2 y)}{1+y \frac{1-x}{x^2}}, \quad y_{\text{th}}^h = s_{\text{th}}^h / m_\mu^2$$

and split $\pi\pi$ below 1 GeV from the rest:

$$(1-x) \bar{\Pi}_{\pi\pi}(t(x)) = -\frac{1-x}{\pi} \int_{y_{\text{th}}^{\pi\pi}}^{y_1} \frac{dy}{y} \frac{\text{Im} \bar{\Pi}_{\pi\pi}(m_\mu^2 y)}{1+y \frac{1-x}{x^2}}, \quad y_1 = (1\text{GeV}/m_\mu)^2$$

HVP contribution to a_μ – from the spacelike region

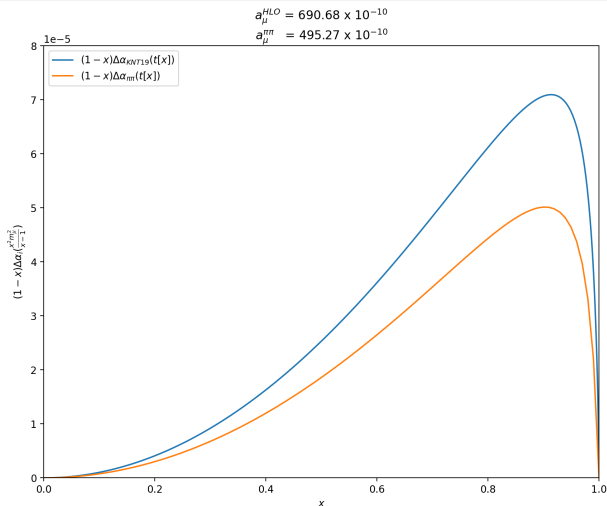


Figure: Full hadronic contribution (blue); $\pi\pi$ -contribution (orange).
 $[\bar{\Pi}(t) = \Delta\alpha(t)]$

HVP contribution to a_μ – from the spacelike region

$\bar{\Pi}_{\text{rest}}(t)$ is small and smooth, we represent it as:

$$\bar{\Pi}_{\text{rest}}(t) = \sum_{\ell=1}^L r_\ell (v(t)^\ell - v(0)^\ell),$$

where the conformal variable v is given by

$$v(t) = \frac{\sqrt{t_{\text{in}} - t_r} - \sqrt{t_{\text{in}} - t}}{\sqrt{t_{\text{in}} - t_r} + \sqrt{t_{\text{in}} - t}}, \quad t_{\text{in}} = 1 \text{ GeV}^2$$

(since the $\pi\pi$ channel is included only up to 1 GeV)

Splitting $\bar{\Pi}_{\text{rest}}(t)$ further still possible if needed

Pseudodata to test our parametrization

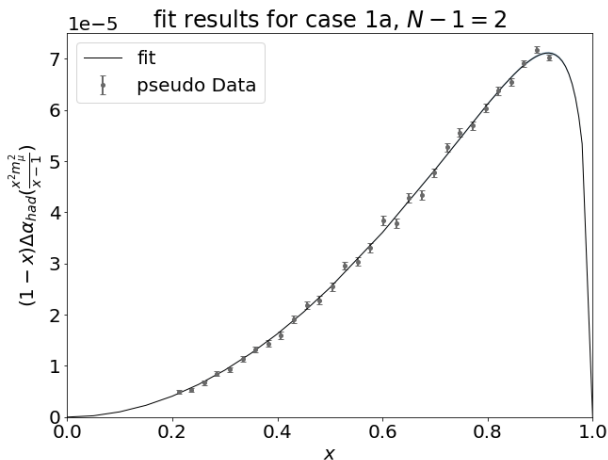


Figure: Pseudo data in range $0.21 < x < 0.92$. [Master Thesis of Barbara Jenny](#)

How we fit them

- ▶ $\pi\pi$ contribution: 4 free parameters
- ▶ rest: 1 free parameter
- ▶ spacelike data cannot determine all of them, nor distinguish $\pi\pi$ from “rest”
- ▶ \Rightarrow add knowledge on $\pi\pi$ parameters from timelike data

$$\begin{aligned}\chi^2(p) &= \chi_1^2(p) + w\chi_2^2(p) \\ &= \sum_i \frac{(y_i - f(x_i, p))^2}{\sigma_i^2} + w \sum_{i,j} (p_i - p_i^0) V_{ij}^0 (p_j - p_j^0),\end{aligned}$$

$w \in [0, 1]$ is a weight parameter

y_i are pseudodata and $f(x_i, p)$ our parametrization, and p_i^0 central values of the $\pi\pi$ parameters from the fit to timelike data (and V_{ij}^0 the corresponding covariance matrix)

Fit dependence on w

Fit to the pseudodata based on KNT19.

Expected value:

$$a_\mu^{\text{HVP, LO}} = 690.68 \times 10^{-10}$$

| w | χ_1 | χ_2 | r_1 | $a_\mu^{\text{HVP, LO}} \times 10^{10}$ |
|------|----------|----------------------|-----------------|---|
| 1 | 38.86 | 4.1×10^{-7} | 0.0096(1)(3)(1) | 691.11(0.20)(0.09)(0.11) |
| 0.1 | 38.86 | 1.7×10^{-5} | 0.0096(1)(3)(1) | 691.11(0.65)(0.09)(0.11) |
| 0.01 | 38.85 | 0.004 | 0.0096(2)(3)(1) | 691.10(2.05)(0.09)(0.10) |
| 0 | 37.90 | $3.6 \times 10^{+6}$ | 0.0017(12) | 688.00(24.48) |

Master Thesis of Barbara Jenny

$w = 0$ gives a completely unphysical $\pi\pi$ contribution

Estimate of statistical uncertainties

The statistical uncertainties have been estimated by generating 100 sets of pseudodata.

Outcome (for $w = 1$):

$$a_{\mu}^{\text{HVP, LO}} = 691.5(2.4)(0.25) \times 10^{-10}$$

with $\chi^2 = 30(7)$ for 25 dof; $r_1 = 9.7(1) \times 10^{-3}$

Relevance of the measurement range in x

Expected value:

$$a_{\mu}^{\text{HVP, LO}} = 690.68 \times 10^{-10}$$

| x range | n. data pts | $a_{\mu}^{\text{HLO}} \times 10^{10}$ |
|-------------------|-------------|---------------------------------------|
| $0.21 < x < 0.92$ | 30 | 691.11(0.20)(0.09)(0.11) |
| $0.25 < x < 0.85$ | 30 | 692.69(0.20)(0.39)(0.25) |
| $0.21 < x < 0.95$ | 31 | 691.50(0.20)(0.29)(0.19) |

Master Thesis of Barbara Jenny

Exact range in x does not appear to be critical

Greynat, de Rafael (22) → talk by D. Greynat

Is the parametrization flexible enough?

To answer this question we have:

1. applied significant distortions to the timelike data
2. generated corresponding spacelike pseudodata
3. fit these with the same parametrization

| | r_1 | $a_\mu^{\text{HLO}} _{\text{expectation}}$ | a_μ^{HLO} |
|--|-----------------|---|--------------------------|
| Resonance at 1.5 GeV^2 | 0.0111(1)(3)(3) | 715.31 | 717.24(0.20)(0.40)(0.39) |
| ψ - Resonance | 0.0108(1)(3)(3) | 708.61 | 710.06(0.20)(0.40)(0.38) |
| Υ - Resonance | 0.0106(1)(3)(3) | 704.80 | 706.20(0.20)(0.40)(0.37) |
| +5%: $\sqrt{s} \in [1, 3] \text{ GeV}$ | 0.0102(1)(3)(3) | 696.98 | 698.94(0.20)(0.40)(0.36) |
| +10%: $\sqrt{s} \in [3, 10] \text{ GeV}$ | 0.0100(1)(3)(3) | 693.45 | 695.27(0.20)(0.40)(0.35) |

Master Thesis of Barbara Jenny

Quality of fits very similar to physical case

To be done

- ▶ Try a fit describing the whole contribution with a conformal polynomial (it works)
- ▶ Play with different parametrizations (Greynat, de Rafael, Padé, lepton-like) to understand possible differences

→ talks by C.Y. London and D. Greynat

- ▶ Provide the codes to the MUonE collaboration
- ▶ Write it up

work in progress, GC, B. Jenny

Outline

Introduction: $(g - 2)_\mu$ in the Standard Model

Lattice vs data-driven approach

Lattice HVP and intermediate window

Data-driven approach

Dispersive approach for the $\pi\pi$ contribution

Spacelike region and MUonE

Master Thesis of Barbara Jenny

Conclusions

Conclusions

- ▶ The HVP contribution is currently the main source of theory uncertainty for a_μ
- ▶ The discrepancy between lattice and the data-driven approach makes this problem even more acute
- ▶ For the **intermediate window** the discrepancy is by now confirmed and represents a **serious puzzle**
- ▶ The **MUonE experiment** could contribute significantly to the resolution of the puzzle
- ▶ A physically-motivated parametrization can successfully fit the **MUonE data**
- ▶ The analysis I have discussed shows that **the limited range in x** is not an obstacle for reaching the **desired accuracy**